Comparison of small polaron migration and phase separation in olivine $LiMnPO_4$ and $LiFePO_4$ using hybrid density functional theory

Shyue Ping Ong,* Vincent L. Chevrier,† and Gerbrand Ceder‡

Department of Materials Science and Engineering, Massachusetts Institute of Technology, 77 Massachusetts Avenue, Cambridge, Massachusetts 02139, USA

(Received 20 October 2010; revised manuscript received 20 January 2011; published 16 February 2011)

Using hybrid density functional theory based on the Heyd-Scuseria-Ernzerhof (HSE06) functional, we compared polaron migration and phase separation in olivine $LiMnPO_4$ to $LiFePO_4$. The barriers for free hole and electron polaron migration in the Mn olivine system are calculated to be 303 and 196 meV, respectively, significantly higher than the corresponding barriers of 170 and 133 meV, respectively, for the Fe olivine system, in agreement with previous experimental findings. These results suggest that the electronic conductivities of $LiMnPO_4$ and $MnPO_4$ are about 177 and 11 times lower than their respective Fe analogs at room temperature. In the presence of lithium vacancies or ions, the barriers for both hole and electron polaron migration were found to be about 100–120 meV higher in the Mn olivine. The HSE06 functional, with its more universal treatment of self-interaction error, was found to be essential to the proper localization of a polaron in the Mn olivine but predicted qualitatively incorrect phase separation behavior in the Li_xFePO_4 system.

DOI: 10.1103/PhysRevB.83.075112 PACS number(s): 71.20.−b, 31.15.E−, 71.38.−k, 82.47.Aa

I. INTRODUCTION

The olivine $LiMPO_4$ family of compounds, where M is typically Fe, Mn, Co, or Ni, are a promising class of cathode materials for rechargeable lithium-ion batteries. $LiFePO_4$[1] has already found widespread applications in industry due to its reasonable theoretical capacity of 170 $mAhg^{-1}$ and voltage of 3.5 V, low cost, low toxicity, and safety. In recent years, there has been increasing interest in the Mn analog, $LiMnPO_4$, which has the higher voltage of 4.1 V vs. Li/Li^+, which is still well within the limitation of existing electrolytes.[2]

However, previous work has identified several potential issues with $LiMnPO_4$, including low ionic and electronic conductivities,[3–5] a high surface energy barrier for Li diffusion,[6] significant volume change at the phase boundary,[3,7,8] and a relatively poor thermal stability of the charged state.[9–11] Kang *et al.*'s attempts to optimize $LiMnPO_4$[12] using a proven off-stoichiometric optimization approach for $LiFePO_4$[13] have also met with limited success, suggesting that there are other intrinsic kinetic limitations compared to $LiFePO_4$.

Previous theoretical work by Maxisch *et al.*[14] and various experimental works[15,16] have provided evidence of a small polaron[17,18] diffusion mechanism of electronic conduction in $LiFePO_4$. Electronic conduction in the structurally similar $LiMnPO_4$ is likely to be via a similar mechanism. Indeed, Yamada *et al.*[3,4] postulated that a large polaron effective mass in the Mn olivine due to the Jahn-Teller active Mn^{3+} ion is the likely explanation for the observed low electronic conductivities. Yamada *et al.* also suggested large local lattice deformation due to Mn^{3+} during phase transformation to be a further factor limiting the intrinsic kinetics in $LiMnPO_4$.

In this work, we investigated the polaron migration and phase separation in $LiMnPO_4$ and $LiFePO_4$ using hybrid density functional theory (DFT) based on the Heyd-Scuseria-Ernzerhof (HSE06) functional.[19–21] Previous theoretical work has shown that the standard local density approximation (LDA) and generalized gradient approximation (GGA) to DFT are generally insufficient to treat electron correlation in the localized d states in transition metal oxides and tend to lead to an overdelocalization of the d electrons.[22–24] A more sophisticated treatment with the application of a Hubbard U term (LDA + U or GGA + U) to penalize partial occupancies in the site-projected d orbitals is needed. For $LiMPO_4$ olivine systems, in particular, GGA + U has been shown to give significantly better descriptions of the electronic structures,[25] which are essential to achieving more accurate predictions of the lithium intercalation potential,[2] phase stability and separation behavior,[26–28] and other properties.

Exact Hartree-Fock (HF) exchange cancels the unphysical self-interaction by construction. As such, hybrid functionals, which incorporate a fraction of exact exchange, can be considered an alternative approach to dealing with the overdelocalization of d orbitals in transition metal ions by conventional semilocal functionals, albeit at a significantly higher computational cost than GGA + U. In recent years, hybrid calculations have seen greater use in solid-state applications, such as the study of redox potentials[29] and polarons in doped $BaBiO_3$[30] and cuprates.[31] The advantage of hybrid functionals over GGA + U is the lack of a species-specific U parameter and, perhaps more importantly, a more universal treatment of the self-interaction error over all species and occupied states rather than specific atomic orbital projections on specific ions.

II. METHODS

A. Small polaron migration

A slow-moving electron or hole in a dielectric crystal induces a local lattice distortion, which acts as a potential well that causes the charge carrier to become self-trapped. The quasiparticle formed by the charge carrier and its self-induced distortion is called a small polaron if the range of the lattice distortion is of the order of the lattice constant. In this work, we adopted the same methodology used by Maxisch *et al.*[14] in their GGA + U study of polarons in the Fe olivine as well as Iordanova *et al.*[32,33] in their study of polarons in

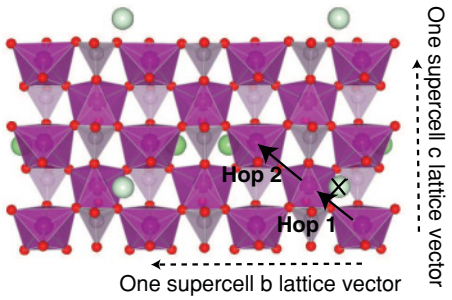

FIG. 1. (Color online) Single layer of an olivine $LiMPO_4$ supercell viewed in projection along the [100] direction, showing polaron hops considered in polaron investigations. The lithium atom marked with the cross is the atom removed when calculating polaron barriers in the presence of vacancies.

oxides. We briefly summarize the methodology here, and interested readers are referred to the work just cited for more details.

The olivine $LiMPO_4$ compounds have an orthorhombic *Pnma* space group where transition metal (M) ions are sixfold coordinated by oxygen ions forming layers of edge-sharing octahedra. Because the layers are separated by PO_4 tetrahedra, we can assume that electron transfer is confined to a single layer, and no charge transfer occurs between layers (hop 1 in Fig. 1). To fulfill the requirements of spin conservation and the Frank-Condon principle, we calculated the polaron migration barriers using an A-type antiferromagnetic structure.[34] A $1 \times 2 \times 2$ supercell containing 16 formula units was used to minimize the interaction between periodic images, while keeping computational costs at a reasonable level.

In $LiMPO_4$, polaronic charge carriers are holes on M^{3+} sites, whereas in MPO_4, the charge carriers are electrons on M^{2+} sites. A hole(electron) polaron was formed on one of the transition metal ions by removing(adding) an electron to the fully relaxed $LiMPO_4$ (MPO_4) supercell. Overall charge neutrality was preserved via a compensating background charge. If $\{\mathbf{q_i}\}$ and $\{\mathbf{q_f}\}$ denote the initial and final ion positions, respectively, the migration of the polaron can then be described by the transfer of the lattice distortion over a one-dimensional Born-Oppenheimer surface, with an energy maximum at a configuration between $\{\mathbf{q_i}\}$ and $\{\mathbf{q_f}\}$. To determine this maximum, we computed the energies for a set of cell configurations $\{\mathbf{q_x}\}$ linearly interpolated between $\{\mathbf{q_i}\}$ and $\{\mathbf{q_f}\}$, that is, $\{\mathbf{q_x}\} = (1-x)\{\mathbf{q_i}\} + x\{\mathbf{q_f}\}$, where $0 < x < 1$.

During the charging or discharging of a battery, lithium or vacancies are injected in the pristine olivine structure, respectively. To study polaron migration in the presence of lithium and vacancies, we introduced a single lithium or vacancy into the supercell and calculated the barrier for the polaron to migrate from an M site nearest to the lithium ion or vacancy to an M site farther away within the same layer (hop 2 in Fig. 1).

B. Phase separation behavior

To study the phase separation behavior of the Mn and Fe olivines, we calculated the formation energies $\Delta E(x)$ of Li_xMPO_4 at $x = 0.25, 0.5, 0.75$, which are given by the following equation:

$$\Delta E(x) = E(\mathrm{Li}_x\mathrm{MPO}_4) - (1-x) \times E(\mathrm{MPO}_4) - xE(\mathrm{LiMPO}_4). \quad (1)$$

For the formation energy calculations, only a single unit cell of $LiMPO_4$ was used, and all symmetrically distinct charge ordering configurations at each concentration were calculated. There is only one symmetrically distinct configuration of Li ions each for $x = 0.25$ and $x = 0.75$. For $x = 0.5$, the lowest energy Li-ion configuration found is when the two Li are at fractional coordinates (0.5,0,0.5) and (0.5,0.5,0.5) in the standard olivine unit cell. The magnetic moments were initialized in the ground-state antiferromagnetic configuration, and the net difference in the number of spin-up and spin-down electrons was fixed at the value expected from the number of M^{2+} and M^{3+} ions present in the structure. For example, for $Li_{0.25}FePO_4$, one of the four Fe ions in the unit cell is a Fe^{2+}, and the remaining Fe ions are Fe^{3+}, resulting in an expected $+1$ net difference in the number of spin-up and spin-down electrons in the unit cell.

C. Computational methodology

All energies were calculated using the Vienna *ab initio* simulation package (VASP)[20] within the projector augmented-wave approach.[35] A plane-wave energy cutoff of 500 eV was used. The hybrid functional chosen was the HSE06[19–21] functional as implemented in VASP. The HSE06 functional is a screened implementation of the PBE0[36] functional, which combines the exchange of the Perdew-Burke-Ernzerhof[37] (PBE) exchange-correlation functional with HF exchange as follows:

$$E_{xc}^{\mathrm{PBE0}} = a_0 E_x^{\mathrm{HF}} + (1-a_0)E_x^{\mathrm{PBE}} + E_c^{\mathrm{PBE}}, \quad a_0 = 0.25, \quad (2)$$

where E_x^{HF} and E_x^{PBE} are the HF and PBE exchange energies, respectively, and E_c^{PBE} is the PBE correlation energy. The HSE06 functional further divides the exchange term into short-range and long-range terms via a screening parameter chosen as a compromise between speed and accuracy, and the long-range exchange is replaced by long-range PBE exchange. This screening procedure reduces the computational cost significantly while achieving an accuracy similar to that of the PBE0 functional.

For polaron supercell calculations, a minimal Γ-centered $1 \times 1 \times 1$ k-point grid was used to keep the computational cost at a reasonable level. No k-point convergence study was done, as any increase in the k-point grid size rendered the computation far too expensive. Nonetheless, given the size of the supercell, we would expect the calculations to be reasonably converged. The single-unit-cell Li_xMPO4 formation energies were calculated using a larger k-point grid chosen such that total energies were converged to within 10 meV/formula unit.

GGA + U calculations were also performed where possible to serve as a basis for comparison. In this work, the rotationally invariant,[24] spherically averaged[38] GGA + U functional, which requires only a single effective interaction parameter U, was used. U values of 4.3 and 4.5 eV were used for Mn

TABLE I. Average M–O bond lengths of polaron and nonpolaron sites in the Mn and Fe olivines in angstroms. Ranges are shown in parentheses for polaron sites.

	Average M–O bond length in $LiMPO_4$ (Å)		Average M–O bond length in MPO_4 (Å)	
	Hole polaron site	Nonpolaron site	Electron polaron site	Nonpolaron site
Mn	2.07 (1.92–2.28)	2.20	2.18 (2.02–2.38)	2.07
Fe	2.06 (1.99–2.13)	2.16	2.13 (1.97–2.26)	2.03

and Fe, respectively, based on values determined previously[39] using a self-consistent linear response scheme.[40] Given that the U parameter was self-consistently determined, this approach to GGA + U can be considered to be a completely first-principles method with no adjustable parameters.

III. RESULTS

A. Polaron bond lengths and electronic structure

Table I summarizes the average M–O bond lengths for polaron and nonpolaron sites in the supercell structures. Although the average polarizations induced by polaron formation appear to be similar for the Mn and Fe systems, the actual lattice distortions are very different, as evidenced by the much wider range of bond distances for both the hole and the electron Mn polarons. This observation may be attributed to the fact that Mn^{3+} is a Jahn-Teller active ion for which orbital degeneracy is usually broken by a distortion of the MO_6 octahedron.[41]

Figure 2 shows the densities of states (DOSs) stacked area plots for the $LiMPO_4$ structures, where we attempted to localize a single hole polaron using HSE06 and GGA + U. For $LiFePO_4$, clear evidence of a localized polaron can be seen in the GGA + U and HSE06 DOSs. Fe^{2+} has a high-spin $t_{2g}^3(\uparrow)t_{2g}^1(\downarrow)e_g^2(\uparrow)$ electronic configuration. Removal of an electron to form a hole polaron should result in a spin-down state being pushed above the Fermi level, which is shown in Figs. 2(c) and 2(d). We also note that the polaron states and the states near the Fermi level have predominantly d character in the Fe olivine.

For $LiMnPO_4$, we were unable to localize a hole polaron using GGA + U. The electronic structure of Mn^{2+} is $t_{2g}^3(\uparrow)$ $e_g^2(\uparrow)$. Removal of an electron to form a hole polaron should result in a spin-up state being pushed above the Fermi level.

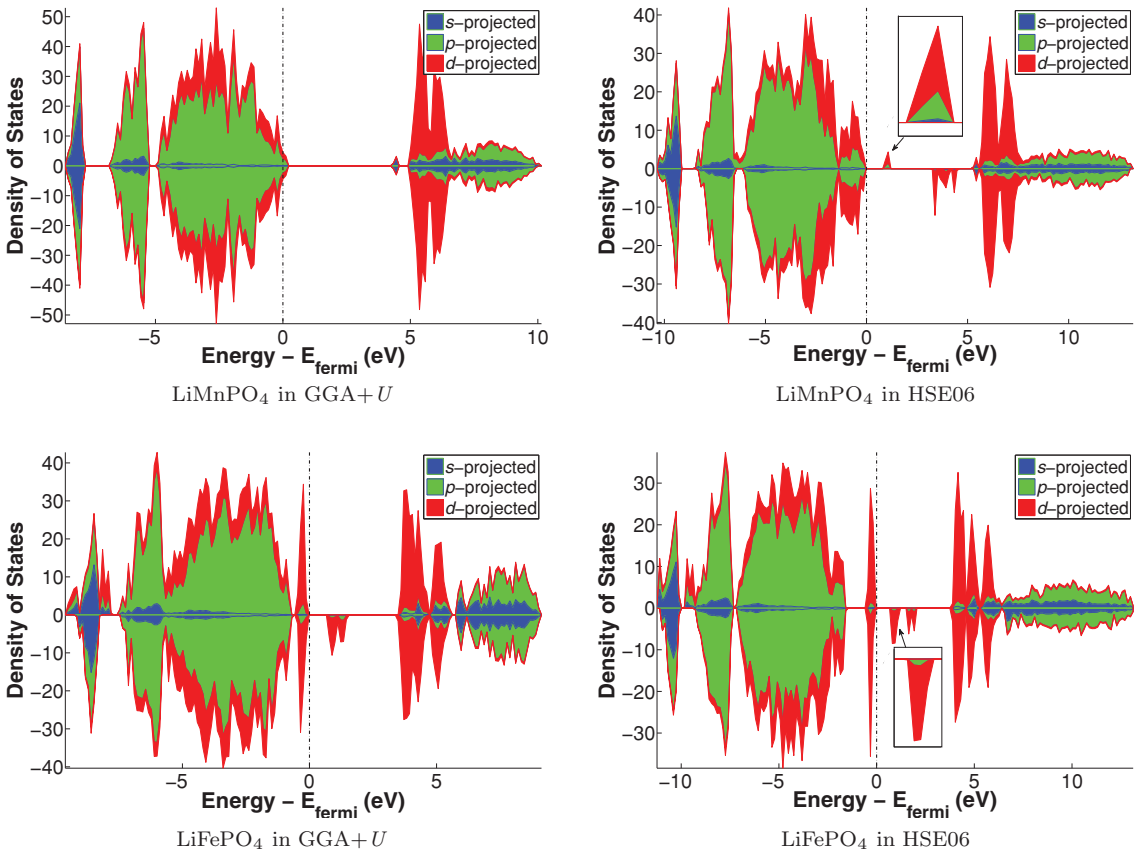

FIG. 2. (Color online) Density of states (DOS) stacked area plots for $LiMPO_4$ olivine containing a single hole polaron. The height of each colored area shows the contribution of each orbital type at each energy level. To obtain a more accurate DOS, a non-self-consistent run using a 2 × 2 × 2 Monkhorst-Pack k-point grid on the structure optimized using the default single Γ point was performed.

No such state was observed in the GGA + U DOS [Fig. 2(a)], while clear evidence of a localized hole polaron in $LiMnPO_4$ was seen in the HSE06 DOS [Fig. 2(b)]. While there are other reports of localized polarons in $LiMnPO_4$ with GGA + U,[42,43] localization in these studies is achieved through the presence of vacancies, and there is no evidence that localized polarons can form with GGA + U in pristine $LiMnPO_4$, where there is no symmetry broken on the Mn sites.

Similar observations were made for electron polaron localization in $FePO_4$ and $MnPO_4$ based on the DOSs (provided in the supplementary material).[44]

The reason for this failure of GGA + U is apparent when we consider the HSE06 orbital-projected DOSs, which clearly shows a significant contribution from the oxygen p orbitals in the polaron states and the states near the Fermi level. This observation points to an inherent difference between the electronic structure of $LiMnPO_4$ and that of $LiFePO_4$; the transition metal is much more strongly hybridized with the nearest-neighbor oxygen atoms in the Mn olivine compared to the Fe olivine. Indeed, the hole polaron charge densities clearly showed a greater localization of charge on the Fe ion in $LiFePO_4$, while the polaron charge carrier appeared to have localized in Mn-d-O-p hybrid orbitals in $LiMnPO_4$ (see supplementary material). In their investigation of polaronic hole trapping in doped $BaBiO_3$, Franchini *et al.*[30] found that they were unable to stabilize a bipolaron using a one-center LDA + U treatment because the Bi s orbitals were too delocalized. In the case of the Mn olivine, we believe that the reason for the failure of GGA + U is different: the relevant localized orbitals in which to apply self-interaction correction are not the on-site atomic transition metal d orbitals but, rather, the hybridized molecular orbitals formed by specific transition metal d orbitals and oxygen p orbitals. To our knowledge, no existing DFT code provides a functionality to apply Hubbard U corrections to nonatomic orbitals. A recent work by Ylvisaker *et al.* applied a novel tight-binding Hamiltonian approach to apply U corrections to molecular oxygen π^* orbitals in RbO_2,[45] but the greater complexity of the olivine structure makes developing a similar model difficult. In this work, we chose to avoid the issue of applying a Hubbard U on hybridized orbitals by using hybrid functionals.

B. Polaron migration barriers

Figure 3 shows the calculated $LiMPO_4$ free hole and MPO_4 free electron polaron migration barriers. For the Fe olivine system, we performed both HSE06 and GGA + U calculations to compare the differences in the predictions between the two treatments of the polaron problem. Only HSE06 results are presented for the Mn system, as we were unable to localize polarons using GGA + U with the self-consistently determined U.

For $LiFePO_4$ and $FePO_4$, the HSE06 polaron migration barriers were smaller than the GGA + U ones. As highlighted in previous work,[29] we found that HSE06 in general tends to result in a smaller amount of charge localization compared to GGA + U. Hence, it is likely that the polaron migration is artificially aided by some residual itinerant character of the charge carriers. The GGA + U migration barriers in this paper

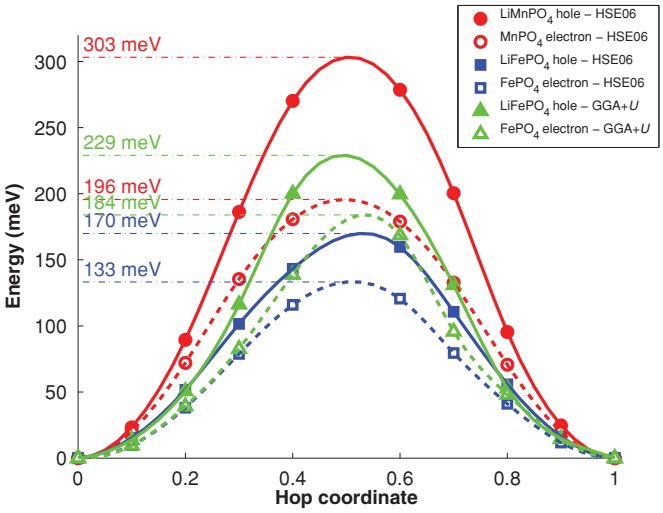

FIG. 3. (Color online) Calculated free polaron migration barriers in HSE06 and GGA + U.

are in good agreement with the values previously calculated by Maxisch *et al.*[14]

Comparing the Mn versus Fe HSE06 barrier values, we see that the free polaron migration barriers in the Mn olivine system are significantly higher than in the Fe olivine. The free hole polaron migration barrier in $LiMnPO_4$ was about 133 meV higher than that in $LiFePO_4$, while the free electron polaron migration barrier in $MnPO_4$ was about 63 meV higher. Such significantly higher polaron migration barriers would imply much lower electronic conductivities in the Mn olivine in both the charged and the discharged state compared to the Fe olivine.

We also investigated the polaron migration barriers in the presence of lithium ions (in MPO_4) or vacancies (in $LiMPO_4$) using the same $1 \times 2 \times 2$ supercell to simulate electronic conduction during the initial stages of charging or discharging. Figure 4 shows the calculated barriers for polaron migration from a site nearest to the lithium ion or vacancy to a site farther away. As we are only interested in relative barriers, we made no

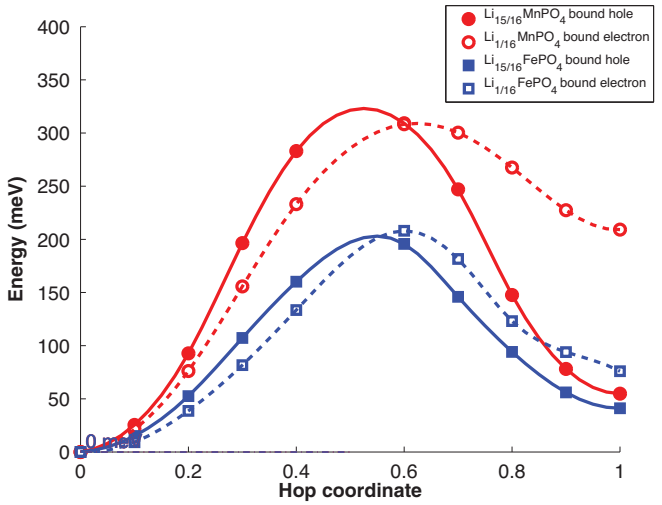

FIG. 4. (Color online) Calculated bound polaron migration barriers in HSE06.

corrections for the interactions between periodic images of the lithium ion or vacancy and charge carriers, as was done in the work by Maxisch *et al.*[14] (because the charges and structures are similar in all instances, the corrections would amount to approximately the same additive term).

We can observe that the bound polaron migration barriers are higher than the free polaron migration barriers. In particular, the electron polaron migration barrier in $Li_{1/16}MnPO_4$ increases significantly, and both hole and electron migration barriers are about 100–120 meV higher in the Mn olivine than the Fe olivine. Hence, polarons have a tendency to become trapped by the presence of lithium ions and vacancies, further reducing electronic conductivity.

In a recent work, Seo *et al.*[42] reported a GGA + U polaron migration barrier of more than 808 meV in Li_xMnPO_4 calculated via a nudged elastic band method and noted this value to be "over 100 meV" higher than the barrier in Li_xFePO_4 calculated by Maxisch *et al.*[14] However, the barrier calculated by Seo *et al.* is for an "undefined" combination of a lithium migration and a polaron migration process and, hence, cannot be compared directly to either Maxisch *et al.*'s work or the barriers calculated in this work. Furthermore, Seo *et al.* used a supercell with an approximate 1/3 Li concentration. Polaron migration barriers under a 1/3 Li concentration are likely to be different from the far more dilute 1/64 concentration investigated by Maxisch *et al.* and 1/16 concentration investigated in this work.

C. Li_xMPO_4 formation energies

The structural evolution of an electrode material upon delithiation can be evaluated by computing the formation energies of states with a lithium content intermediate between the lithiated and the fully delithiated states. The formation energy of $LixMPO_4$, $\Delta E(x)$, is its energy minus the concentration weighted average of MPO_4 and $LiMPO_4$. A large positive $\Delta E(x)$ indicates that no intermediate phases form and a two-phase reaction is likely, while a negative $\Delta E(x)$ indicate the presence of ordered Li-vacancy solid solutions.

Figure 5 presents the formation energies of Li_xMPO_4 calculated using different functionals. In agreement with the previous work by Zhou *et al.*,[26] standard GGA led to qualitatively incorrect negative or near-zero formation energies for the intermediate phases in the Li_xMPO_4 system. Both $LiFePO_4$ and $LiMnPO_4$ are well known to undergo a two-phase reaction upon delithiation,[1,3] implying that the formation energy should be positive. GGA + U with the self-consistently determined U gives positive formation energies. Zhou *et al.* have conclusively shown that accounting for the correlation between the localized d orbitals of the transition metal is necessary to obtain this phase separating behavior. We would like to note that the GGA + U formation energy for $Li_{0.5}FePO_4$ we calculated (≈13 meV) is much lower than the value reported for $U = 4.5$ eV (≈80 meV) in Ref. 26 but is very close to the lowest formation energy for the same structure reported in a later work by the same author[46] for a set of 245 calculated structures used to fit a cluster expansion.[27]

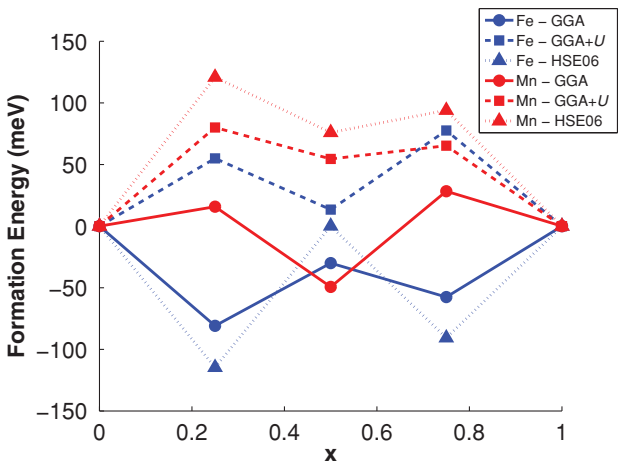

FIG. 5. (Color online) Formation energies of Li_xMPO_4 using different functionals.

The HSE06 formation energies for the Li_xMnPO_4 structures are higher than the GGA + U values and predicts qualitatively correct phase separating behavior.

However, the results of the HSE06 Li_xFePO_4 formation energies are surprising. We would expect that a functional that is designed to explicitly treat the self-interaction error would result in at least qualitatively correct formation energies. As shown in Fig. 5, the HSE06 formation energies for Li_xFePO_4 for $x = 0.25, 0.75$ are even more negative than the GGA formation energies. This is despite our having achieved the proper charge localization for these structures; that is, the final magnetic moments of the Fe ions confirmed that $Li_{0.25}FePO_4$ contains one Fe^{2+} and three Fe^{3+} ions, while $Li_{0.75}FePO_4$ contains one Fe^{3+} and three Fe^{2+} ions (see supplementary material).

IV. DISCUSSION

A. Intrinsic kinetic differences between the Mn and the Fe olivines

Our results show that there are intrinsic differences in the electronic structures and kinetics of $LiMnPO_4$ and $LiFePO_4$. The free hole and electron polaron migration barriers in the Mn olivine are predicted to be 133 and 63 meV higher than those in the Fe olivine, respectively. In the presence of lithium ions or vacancies, both the hole and the electron polaron migration barriers are ≈100–120 meV higher in the Mn olivine relative to the Fe olivine. In terms of the formation energies of the partially lithiated $LiMPO_4$ structures, we found that the Mn and Fe systems had approximately the same formation energies in GGA + U and that the HSE06 formation energies for the Mn olivine were similar to the GGA + U values.

Using the calculated polaron migration barriers, we may make an approximation to the difference in electronic conductivities between the Mn and the Fe olivines. Assuming the same attempt frequency and a simple Arrhenius-like relationship, the *free hole polaron migration is predicted to be about 177 times slower in $LiMnPO_4$ than in $LiFePO_4$ at room temperature, while the electron polaron migration is predicted to be about 11 times slower in $MnPO_4$ than in $FePO_4$*. In the presence of Li ions or vacancies, both hole and electron migration are predicted to be about 77 times slower in the Mn olivine compared to the Fe olivine. These predictions are in good agreement with the results of Yonemura *et al.*,[4]

who measured conductivities of $<10^{-10}$ Scm^{-1} for $LiMnPO_4$ compared to 10^{-8} Scm^{-1} for $LiFePO_4$. It should be noted that there are some discrepancies in the literature. For instance, Delacourt *et al.*[5] found that $LiMnPO_4$ had a conductivity 5 orders of magnitude lower, which implies an activation energy a factor of 2 higher, compared to $LiFePO_4$. Nonetheless, the qualitative assessment that the Mn olivine has a much lower electronic conductivity still stands.

There are several implications of the much lower conductivity for $LiMnPO_4$ relative to $LiFePO_4$. First, size effects would be far more pronounced, and indeed Drezen *et al.*[47] found that a reduction in particle size from 270 to 140 nm significantly improved the rate capability of $LiMnPO_4$ as an electrode, and even better performance was subsequently achieved by Martha *et al.*[48] with carbon-coated 30-nm particles. It should be noted that carbon coating merely improves interparticle conductivity, and not intraparticle conductivity; hence a small particle size is still necessary to achieve low transport distances. If the requisite particle sizes to achieve a similar performance as $LiFePO_4$ are significantly smaller, the overall effective gravimetric and volumetric capacity of the cathode could be adversely affected, and the potential thermal stability issues in the charged state[9–11] could be further exacerbated.

The GGA + U formation energies for states with an intermediate lithium concentration in the Fe and Mn olivine are similar and consistent with the observed two-phase equilibria in both systems. The HSE06 formation energies were too unreliable for us to make any reasonable assessment. While we are unable to provide a quantitative discussion of the phase separation kinetics in the olivines, we note two observations from our work that may point to slower phase separation kinetics in $LiMnPO_4$. First, lower electronic conductivities arising from higher polaron migration barriers in the Mn olivine may impede phase transformation because both Li and electrons must diffuse to the site of transformation for phase transformation to occur. Second, the greater lattice mismatch between the delithiated and the lithiated phases of the Mn olivine suggests that nucleation barriers in the the Mn olivine are likely to be higher than in the Fe olivine due to higher coherency strain at the phase transformation interface.

B. Successes and limitations of HSE06 versus GGA + U

Beyond the insights into the differences between the Mn and the Fe olivines, our investigations also highlighted the successes and limitations of the HSE06 hybrid density functional versus the conventional DFT functional based on GGA + U. On one hand, the HSE06 functional was essential in achieving a proper localization of the polaron in the more strongly hybridized Mn olivine system, where the GGA + U was unable to achieve such a localization. On the other, it failed to predict even qualitatively correct formation energies for Li_xFePO_4. Our results suggest that while the HSE06 functional provides a more universal treatment of self-interaction over all atomic species, its treatment of electron correlation in strongly localized transition metal states such as those in the Fe olivine is still deficient. This deficiency is likely to be present in all hybrid functionals derived from PBE0 with a 0.25 fraction of exact exchange.

Despite this noted failure and the significantly higher computational costs, we believe that the more universal approach to treating self-interaction offered by hybrid functionals such as HSE06 is important in capturing the essential physics of systems with strongly hybridized localized states that are not captured in current formulations of DFT + U. But our results also show that the hybrid functionals in their current state of development cannot be regarded as a panacea to self-interaction error correction, and in some systems, DFT + U provides a better qualitative description.

V. CONCLUSION

In this work, we have studied polaron migration and phase separation in olivine $LiMnPO_4$ and $LiFePO_4$ using hybrid DFT based on the HSE06 functional. The barriers for free hole and electron polaron migration in the Mn olivine system are 133 and 63 meV higher than those in the Fe olivine system, respectively, suggesting 177 times slower electronic conduction in $LiMnPO_4$ and 11 times slower electronic conduction in $MnPO_4$ relative to the Fe analogs. In the presence of lithium vacancies or ions, the barriers for both hole and electron polaron migration were found to be about 100–120 meV higher in the Mn olivine. The HSE06 functional, with its more universal treatment of self-interaction error, was found to be essential to the proper localization of a polaron in the Mn olivine but predicted qualitatively incorrect phase separation behavior in the Li_xFePO_4 system.

ACKNOWLEDGMENTS

This work was supported by the US Department of Energy under Contract No. DE-FG02-96ER45571 and the BATT program under Contract No. DE-AC02-05CH11231.

*Corresponding author: shyue@mit.edu
†vchev@mit.edu
‡gceder@mit.edu; http://ceder.mit.edu

[1] A. Padhi, K. Nanjundaswamy, and J. Goodenough, J. Electrochem. Soc. **144**, 1188 (1997).
[2] F. Zhou, M. Cococcioni, K. Kang, and G. Ceder, Electrochem. Commun. **6**, 1144 (2004).
[3] A. Yamada, Y. Kudo, and K.-Y. Liu, J. Electrochem. Soc. **148**, A1153 (2001).
[4] M. Yonemura, A. Yamada, Y. Takei, N. Sonoyama, and R. Kanno, J. Electrochem. Soc. **151**, A1352 (2004).
[5] C. Delacourt, L. Laffont, R. Bouchet, C. Wurm, J.-B. Leriche, M. Morcrette, J.-M. Tarascon, and C. Masquelier, J. Electrochem. Soc. **152**, A913 (2005).
[6] L. Wang, F. Zhou, and G. Ceder, Electrochem. Solid State Lett. **11**, A94 (2008).
[7] A. Yamada and S.-C. Chung, J. Electrochem. Soc. **148**, A960 (2001).

[8]N. Meethong, H.-Y. Huang, S. Speakman, W. Carter, and Y.-M. Chiang, Adv. Funct. Mater. **17**, 1115 (2007).
[9]S.-W. Kim, J. Kim, H. Gwon, and K. Kang, J. Electrochem. Soc. **156**, A635 (2009).
[10]G. Chen and T. J. Richardson, J. Power Sources **195**, 1221 (2010).
[11]S. P. Ong, A. Jain, G. Hautier, B. Kang, and G. Ceder, Electrochem. Commun. **12**, 427 (2010).
[12]B. Kang and G. Ceder, J. Electrochem. Soc. **157**, A808 (2010).
[13]B. Kang and G. Ceder, Nature **458**, 190 (2009).
[14]T. Maxisch, F. Zhou, and G. Ceder, Phys. Rev. B **73**, 104301 (2006).
[15]K. Zaghib, A. Mauger, J. B. Goodenough, F. Gendron, and C. M. Julien, Chem. Mater. **19**, 3740 (2007).
[16]B. Ellis, L. K. Perry, D. H. Ryan, and L. F. Nazar, J. Am. Chem. Soc. **128**, 11416 (2006).
[17]C. G. Kuper and G. D. Whitfield, eds., *Polarons and Excitons* (Oliver & Boyd, Edinburgh, 1962).
[18]H. Fröhlich, Adv. Phys. **3**, 325 (1954).
[19]J. Heyd, G. E. Scuseria, and M. Ernzerhof, J. Chem. Phys. **118**, 8207 (2003).
[20]J. Heyd, G. E. Scuseria, and M. Ernzerhof, J. Chem. Phys. **124**, 219906 (2006).
[21]J. Paier, M. Marsman, K. Hummer, G. Kresse, I. C. Gerber, and J. G. Angyán, J. Chem. Phys. **124**, 154709 (2006).
[22]V. I. Anisimov, I. V. Solovyev, M. A. Korotin, M. T. Czyzyk, and G. A. Sawatzky, Phys. Rev. B **48**, 16929 (1993).
[23]V. I. Anisimov, J. Zaanen, and O. K. Andersen, Phys. Rev. B **44**, 943 (1991).
[24]A. I. Liechtenstein, V. I. Anisimov, and J. Zaanen, Phys. Rev. B **52**, R5467 (1995).
[25]F. Zhou, K. Kang, T. Maxisch, G. Ceder, and D. Morgan, Solid State Commun. **132**, 181 (2004).
[26]F. Zhou, C. A. Marianetti, M. Cococcioni, D. Morgan, and G. Ceder, Phys. Rev. B **69**, 201101 (2004).
[27]F. Zhou, T. Maxisch, and G. Ceder, Phys. Rev. Lett. **97**, 155704 (2006).
[28]S. P. Ong, L. Wang, B. Kang, and G. Ceder, Chem. Mater. **20**, 1798 (2008).
[29]V. L. Chevrier, S. P. Ong, R. Armiento, M. K. Y. Chan, and G. Ceder, Phys. Rev. B **82**, 075122 (2010).
[30]C. Franchini, G. Kresse, and R. Podloucky, Phys. Rev. Lett. **102**, 256402 (2009).
[31]C. H. Patterson, Phys. Rev. B **77**, 094523 (2008).
[32]N. Iordanova, M. Dupuis, and K. M. Rosso, J. Chem. Phys. **123**, 074710 (2005).
[33]N. Iordanova, M. Dupuis, and K. M. Rosso, J. Chem. Phys. **122**, 144305 (2005).
[34]E. O. Wollan and W. C. Koehler, Phys. Rev. **100**, 545 (1955).
[35]G. Kresse and J. Furthmuller, Phys. Rev. B **54**, 11169 (1996).
[36]C. Adamo and V. Barone, J. Chem. Phys. **110**, 6158 (1999).
[37]J. P. Perdew, K. Burke, and M. Ernzerhof, Phys. Rev. Lett. **77**, 3865 (1996).
[38]S. L. Dudarev, G. A. Botton, S. Y. Savrasov, C. J. Humphreys, and A. P. Sutton, Phys. Rev. B **57**, 1505 (1998).
[39]F. Zhou, M. Cococcioni, C. A. Marianetti, D. Morgan, and G. Ceder, Phys. Rev. B **70**, 235121 (2004).
[40]M. Cococcioni and S. de Gironcoli, Phys. Rev. B **71**, 035105 (2005).
[41]C. Marianetti, D. Morgan, and G. Ceder, Phys. Rev. B **63**, 224304 (2001).
[42]D.-H. Seo, H. Gwon, S.-W. Kim, J. Kim, and K. Kang, Chem. Mater. **7**, 091223161926007 (2009).
[43]Z. X. Nie, C. Ouyang, J. Z. Chen, Z. Y. Zhong, Y. L. Du, D. S. Liu, S. Q. Shi, and M. S. Lei, Solid State Commun. **150**, 40 (2010).
[44]See supplemental material at [http://link.aps.org/supplemental/10.1103/PhysRevB.83.075112] for polaron charge densities, MPO4 density of states plots, and calculated magnetic moments of LixMPO4.
[45]E. R. Ylvisaker, R. R. P. Singh, and W. E. Pickett, Phys. Rev. B **81**, 180405 (2010).
[46]F. Zhou, Ph.D. thesis, Massachusetts Institute of Technology 2006.
[47]T. Drezen, N.-H. Kwon, P. Bowen, I. Teerlinck, M. Isono, and I. Exnar, J. Power Sources **174**, 949 (2007).
[48]S. K. Martha, B. Markovsky, J. Grinblat, Y. Gofer, O. Haik, E. Zinigrad, D. Aurbach, T. Drezen, D. Wang, G. Deghenghi, and I. Exnar, J. Electrochem. Soc. **156**, A541 (2009).